UNITED NATIONS UNIVERSITY
UNU-GTP
Geothermal Training Programme

Orkustofnun, Grensasvegur 9,
IS-108 Reykjavik, Iceland

Reports 2014
Number 21

PREDICTING OUTPUT CURVES FOR DEEP WELLS IN THE ASAL RIFT, DJIBOUTI

Miyir Mohamed Abdillahi
Ministry of Energy in Charge of Natural Resources
Immeuble Marabout;
P.O. Box 10010, Djibouti
REPUBLIC OF DJIBOUTI
miyirmed@gmail.com

ABSTRACT

Decade's long combined effort of various surface exploration campaigns and deep drilling has confirmed the existence of a high-temperature geothermal anomaly within the Asal Rift in Djibouti. Several km2 of at least 1 km thick 240-350°C saline resource hosted in a basaltic extensional rift environment is seen. The high scaling potential of the very salty geothermal fluid encountered at depth is however a potential show stopper for long term operations. This is seen as rapid wellbore scaling deposition on the order of 3 cm/year. By doing a numerical wellbore model, calibrated with field data gathered earlier in well A-3 in the Asal Rift, a large 13⅜" casing well design appears amongst the straightest forward scaling mitigation options. Coupled with a decision to operate future Asal Rift wells at wellhead pressures of 20 bars or more. The wellbore model infers a more beneficial wellhead output curve if a reservoir volume hotter than the current 260°C of well A-3 can be intersected. One interesting option in continuing the Asal Rift steam field development is therefore to drill a large diameter, ~2000 m deep directional well from A-3 towards the ~300°C temperature measured in well A-4. Thereby intersecting the presumable near-vertical fracture-dominated permeability of the rift zone, tapping the proven permeability in wells A-3 and A-6 right under the casing shoe and, ideally, finding more permeability at deeper and hotter levels in the bedrock near well A-4. As the reservoir near A-3 was suffering long term pressure drawdown due to the presumably tight outer reservoir boundaries, reinjection should be part of the steam field management strategy. Ideally, one or two successful wells drilled from A-3 towards A-4 can be used for early 5-10 MW production and then some of the older existing wells near A-3 for injection.

1. INTRODUCTION

Thanks to an exceptional geodynamic location, characterized by an emerged triple junction of the Red Sea, Gulf of Aden and East African Rifts, Djibouti hosts an undeveloped geothermal potential which has been explored since 1970. Unfortunately, the exploration has been interrupted many times by political, economic and technical reasons. Therefore, fossil fuel is currently used for power generation. A clean geothermal energy would constitute a key sector for economic and social development, assisting the country in alleviating poverty. Since 2011, a new campaign of exploration under international

financing and expertise has taken place. The new project aims to drill 4 wells in the Asal Region for an expected electrical production of 50 MW in the first phase. The technical issue of rapid downhole scaling depositions during discharge is, however, a main challenge of the project.

The objective of the current study is to predict wellhead output curves of new wells adapted to a high-salinity geothermal field like those found in Asal, Djibouti, and Reykjanes, Iceland. Eighteen scenarios of various well diameter, feedzone enthalpy and pressure are studied for well output from new and scale-free wells. The time impact of cumulative downhole scaling build-up on their output will also be studied. A wellbore simulator called Hola, calibrated with existing data collected during the long term production test of well Asal 3 was used to generate the possible output curves of a new enhanced well. Finally, a new well location will be proposed by incorporating all three characteristics, i.e. well diameter, the reservoir pressure and enthalpy.

2. GEOLOGICAL SETTING OF DJIBOUTI

The East African rift system (EARS) is a succession of rift valleys that extend over approximately 4000 km from the Afar Triangle in the north to Beira in Mozambique in the south. The EARS is a continental branch of the worldwide mid-ocean rift system. It includes the three major extensional structures: the Afar Depression, the Red Sea, and the Gulf of Aden, generally called the triple junction.

Djibouti is located in the eastern part of Africa at the junction of the plates (Figure 1). In Djibouti, areas of strong geothermal manifestations are located within the Asal and Hanle rifts in the Afar Depression. The surface manifestations appear to be fracture controlled and occur within the recent volcanic and sedimentary rocks or at the contact of recent and old formations (Jalludin, 2003).

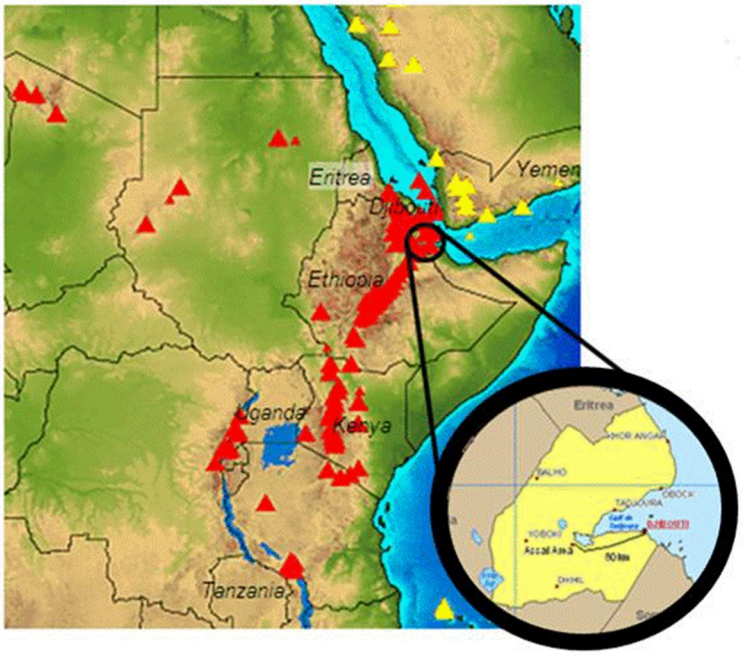

FIGURE 1 : East African Rift, with enlarged view of Djibouti (Smithonian Intsitution, 2013); red triangles are active volcanoes

Figure 2 shows the geological settings of Djibouti in more detail (Elmi, 2005). Djibouti is characterized by largely Miocene to Holocene volcanic rocks and more recent alluvial deposits. Stratoid Series (1.5-3.5 My) cover the major part of the country, mainly in the central and western parts along a S-N axis. The northern part of Djibouti is characterized by volcanic formations of late Miocene age, with extensive and deeply faulted Mabla rhyolites (12-8 My) partly covered by Basalt of Dalha (7-4 My) gently dipping to the northwest. This geologic block is rather stable and appears to be a part of the Arabic Plate since oceanic spreading stopped along the Bab-El-Mandeb straight of the Red Sea and developed inside Afar for the last 3 to 4 My (Marinelli and Varet, 1973). Insignificant high-enthalpy geothermal potential is, therefore, expected there. On the western flank of this block, however, the Dalha Plateau sinks under the more recent basalts of the Stratoid series, itself deeply faulted. Near the triple state boundary with Ethiopia and Eritrea, an active axial range called Manda-Inakir was identified (Haga et al., 2012). Since then, the huge N-S fault zone linking Manda-Inakir and Asal Rift segments was interpreted as the surface

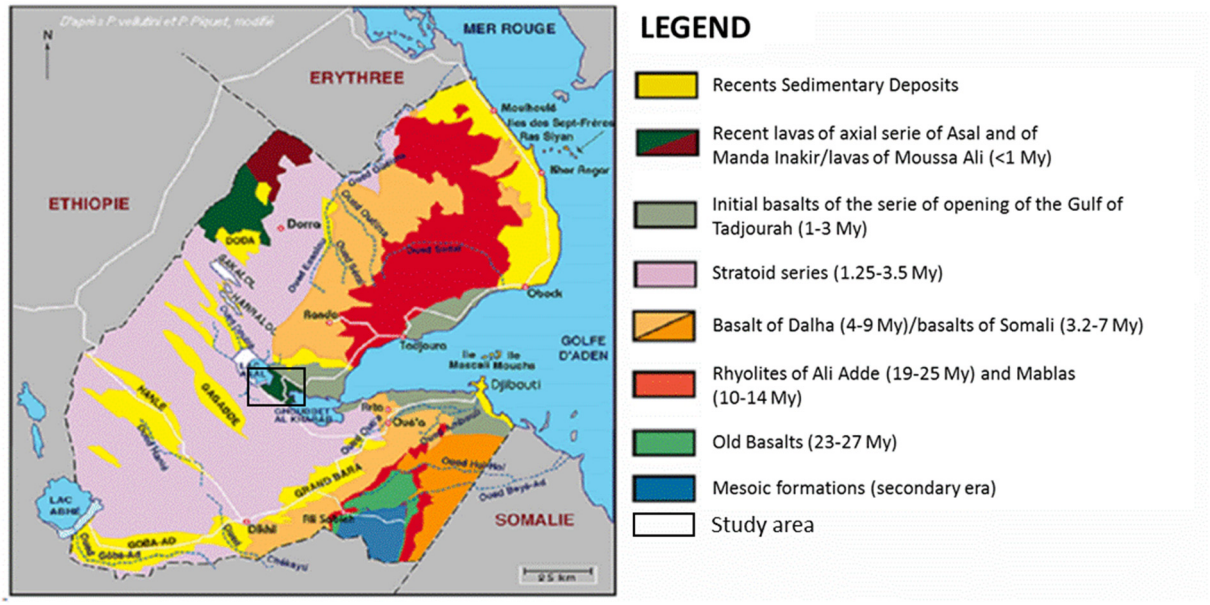

FIGURE 2 : Geological map of Djibouti (Elmi, 2005)

expression of a transform fault (Tapponier and Varet, 1974). Hence, an active plate boundary crosses through the westernmost part of this region, with a related geothermal heat source. The north is characterized by the recent basalt of Dalha (4-9 My), and rhyolite (19-25 My).

According to the Geothermal Energy Association (Omenda, 2008), the geothermal energy potential in Djibouti is estimated as 230-860 MWe based on prospects of the mains regions of the country such as Lake Abbe, Hanle, Gaggade – in the region of Tadjourah, Dorra – in the region of Obock, and Arta in the region of Arta.

The Asal geothermal area is located on an active rift zone that extends from the Ghoubbet Al-Kharab through Lake Asal, into the mountain range northwest of the lake and up through the Alol plains. The rift is also active on the northern shore of Ghoubbet Al-Kharab which represents the landward prolongation of the oceanic spreading axis of the Gulf of Aden and is bounded by two systems of opposite-facing faults (Battistelli et al., 1991). Figure 3 shows the field location and topographic features of the existing well field. This area has been explored for many years, mainly by French scientists, inspired by this very impressive northwest-southeast trending fault system. As Lake Asal is the lowest place in Africa, 153 m below sea level, there is a steady flow of seawater from the sea through the 10 km wide volcanic area between Ghoubbet Al-Kharab and Lake Asal. This flow goes mainly through the northern part of the area where tectonic movement is still active. The inflow has been estimated to be on the order of 20 m^3 per second. In spite of this inflow, there are many fumaroles in the area and it is clear that the temperature below that is heating the lateral cold inflow toward Lake Asal must be very high.

3. DATA SOURCES

3.1 The Asal Rift drilling campaign

The Asal rift, initially explored in the 1960s, is an intensely faulted terrain that separates Lake Asal and Ghoubbet el Kharab. It is the northwest propagation of the Gulf of Aden Rift into the Afar Triple Junction. It can be viewed as an asymmetric rift within the rift structure with the internal rift being the most recent structural development of the region. The Asal geothermal field is hosted by this rift. The

outer rift extends southwest from the Loynoytali faults. The inner rift where the most recent tectonic and volcanic activity is concentrated extends between the Loynoytali faults in the southwest to the northeast Asal rift margin. Rift development took place on terrain made up of Afar stratoid series basalts (4-1 My) and is believed to have been initiated about 3.4 million years ago. The rift margins and floor are made up of rocks of the Asal series basalts that range in age between 0.7 My and present. They are basaltic in composition and were produced by three forms of eruption: sub-aqueous eruptions which produced large volumes of hyaloclastites commonly forming volcanic ring structures; the dominant fissure eruptions which produced the lava flows which cover the rift floor; and central eruptions that form the volcanic edifices such as the Fiale volcanic complex. The latest stage of magmatism continues to the present day as illustrated by the birth of a new volcano, Ardoukoba, in 1978. On account of this geological situation, the geothermal gradient is particularly high in the Asal Rift region. That is why this region was chosen for the implementation of geothermal energy projects. Very recent volcanic rocks dominate the Asal Rift region (MERN, 2004).

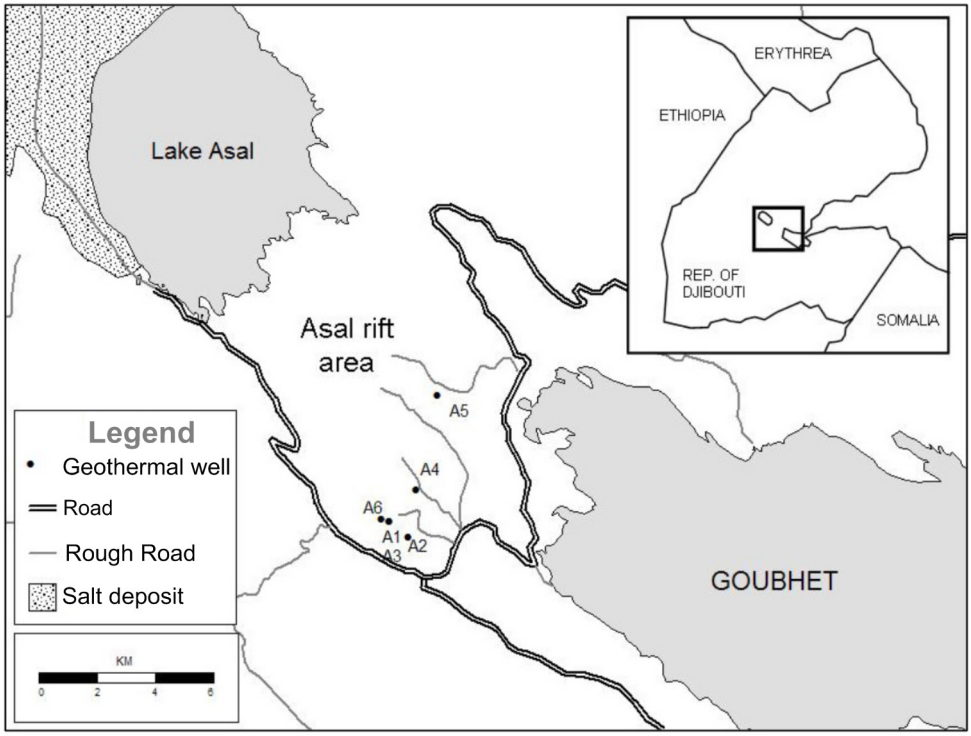

FIGURE 3 : Location of geothermal boreholes in the Asal Rift area
(Elmi, 2005)

Three geothermal sectors have been suggested in the region of Tadjourah. These are named Gale le Goma, Fiale and South of the Lake Asal. The Asal area exploration began in 1975 with the drilling of two deep wells: A-1 and A-2 (BRGM, 1975; BRGM, 1980). Well A-1 had a final depth of 1154 m and well A-2 had a final depth of 1554 m. Well A-1 was able to produce 22 kg/s of high-salinity water. The measured maximum downhole temperature at 1040 m was 255°C before the flow tests, and 260°C during the flow test in 1981. Unfortunately, well A-2 is plugged inside the casing, possibly by drilling mud, and is not producing any steam. The water produced by well A-1 had a very high solids concentration of 128,000 mg/l. During its 1981 flow test, downhole scaling plugged the well in less than 3 months. New holes drilled in the area between Lake Asal and Ghoubbet Al-Kharab, about 10 km northeast of wells A-1 and A-2, were therefore suggested for continuation of the project, primarily because they might have better production characteristics than wells A-1 and A-2. Ideally, these would be similar to wells drilled in the Reykjanes field in Iceland: plain seawater inflow through an active basaltic rift zone (Jónsson, 1985).

In 1987/1988 six additional deep geothermal wells were drilled in Djibouti (Table 1). The first two wells, Hanle 1 and Hanle 2, were drilled in the plain of Hanle to 1623 and 2038 m depth, respectively. Unfortunately, they showed a maximum temperature of only 124°C at 2020 m. This site was consequently put on hold for further development. Instead, four additional wells were drilled in the Asal area (A-3, A-4, A-5 and A-6). Two of them, wells A-3 and A6, that are located close to the southwest margin of the rift, were productive (Figure 3). Their maximum temperatures recorded were 253°C and 265°C, respectively. Wells A-4 and A-5, drilled closer to the centre rift zone, were characterized by high temperatures, up to 350°C at 2100 m in well A-5. Unfortunately, these wells are not productive. Figure 4 shows the well temperatures.

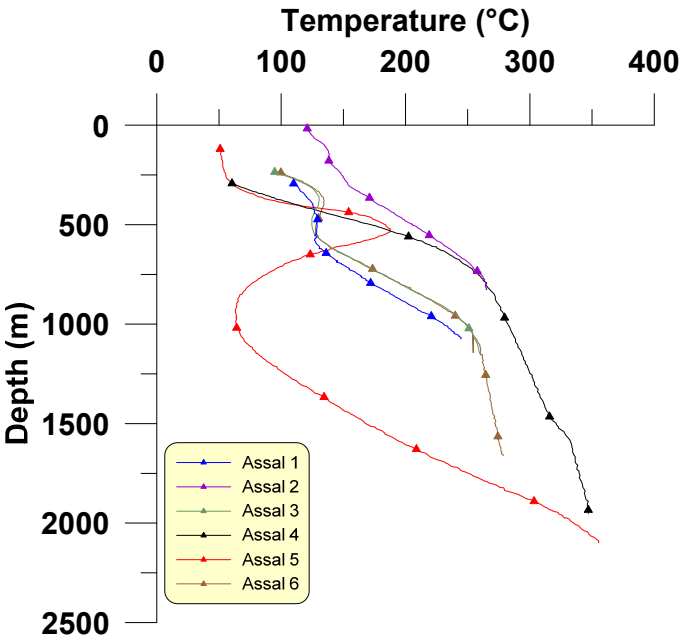

FIGURE 4 : Temperature profiles for all wells in the Asal Rift

The Asal Rift drilling operations was carried out under the technical supervision of Aquater (Aquater, 1988). On the basis of drilling wells A-4 and A-5 both hot but tight, a resistivity survey was done by Orkustofnun - the National Energy Authority of Iceland, delivered after the completion of well A-6 (Árnason and Flóvenz, 1995). This work was later revisited by Reykjavik Energy Invest and a new drilling phase was planned but was not realised due to the financial crisis that hit the world in late 2008 (Hjartarson et al., 2010).

TABLE 1: Status on drilled wells in Asal and Hanle Plain

Well	Total depth (m)	Max temperature (°C)	Status
A-1	1154	260	Productive, scale plug in well
A-2	1554	////	Plugged by drilling mud
A-3	1316	265	Productive
A-4	2011	344	Non-productive but hot
A-5	2105	359	Non-productive but hot
A-6	1761	281	Productive
Hanle 1	1623	72	Non-productive and cold
Hanle 2	2038	123	Non-productive and cold

Drilling of deep wells in the Asal Rift area revealed the existence of several aquifers at depths from 350 to 600 m, with salinity increasing with depth. Sphalerite and galena scaling were also observed in the wells, starting at the flash level at about 850 m depth (D'Amore et al., 1997).

3.2 Static temperature and pressure profiles in well A-3

Temperature and pressure data in well A-3 have been collected over the period of a long term production test. Figure 5 shows the static pressure and temperature profiles of the well, collected after thermal recovery but prior to the 3½ months of production testing. Theses profiles describe the static temperature and pressure profiles of the well below 300 m with a good approximation. Above that, the temperature

profiles were altered by boiling of the brine in the vicinity of the liquid level and by the presence of steam above that (Aquater, 1988). These data are used in a later section to calibrate a numerical model for the well.

3.3 Dynamic pressure and temperature profiles in well A-3

Dynamic downhole temperature and pressure field data, collected during a long-term production test of well A-3 at different dates, are presented below (Figures 6-8). Main results from the test were summarised as (Aquater, 1988):

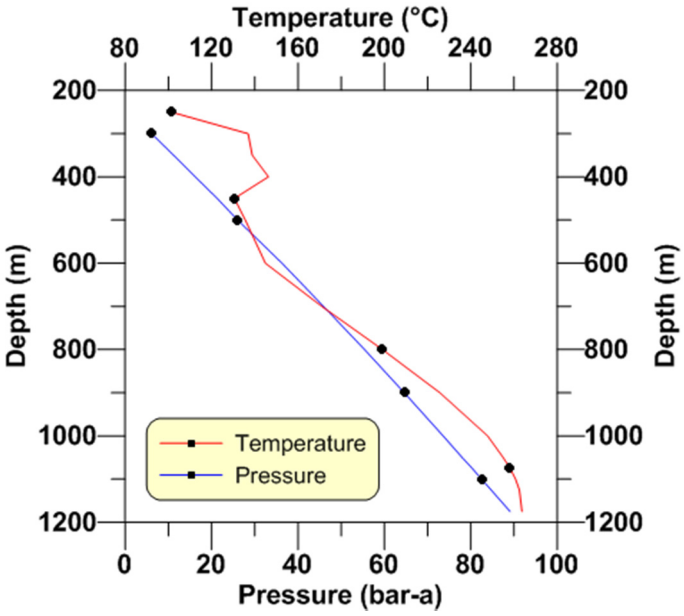

FIGURE 5: Static temperature and pressure profiles in well A-3

- A decline on the reservoir pressure of 3.5-4 bar in the first period of increased production;
- An increase in the fluid temperature from 263 to 265°C at the wellbore and from 259 to 263°C at the flashing point;
- An increase of the MDP (Maximum Discharge Pressure) and a sizeable reduction in productivity at lower wellhead pressures (from 111 to 63 kg/s).

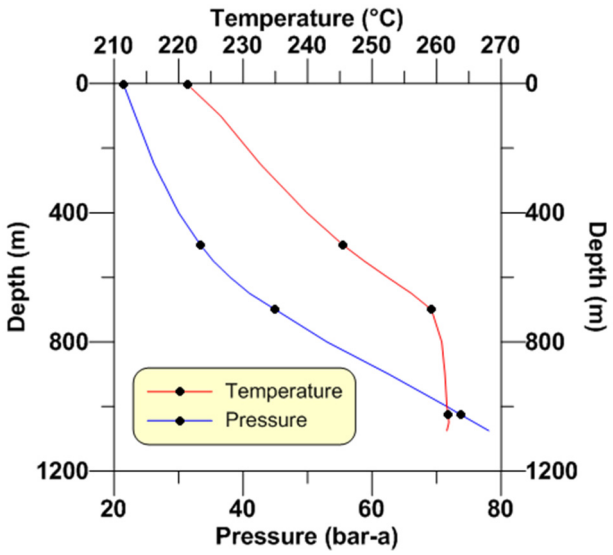

FIGURE 6: Well A-3 dynamic profiles at 26.3 kg/s (09/04/1987)

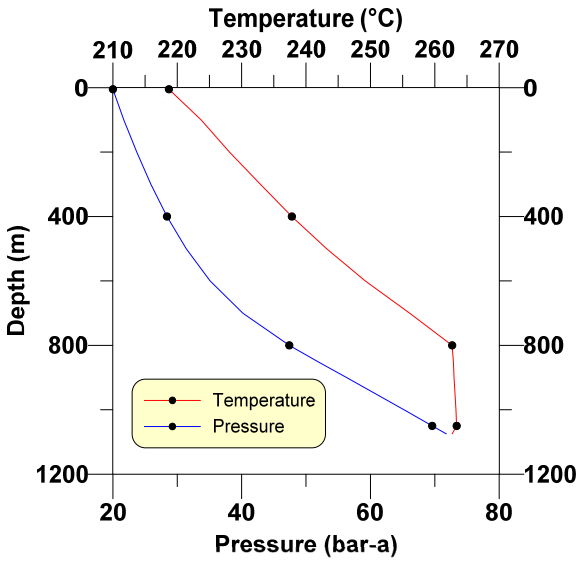

FIGURE 7: Well A-3 dynamic profiles at 49 kg/s (10/14/1987)

3.4 Caliper logs

Due to the high scaling potential of fluid coming to well A-3, a reduction of the wellbore diameter of 1.5 cm at the wellhead and 2 cm at the flashing point (Aquater, 1988) was observed by a caliper log (). The latter depth corresponds both to the deeper limit of scale deposits as detected by the caliper log, and to the approximate lower limit of flashing as seen in Figures 6-8. The caliper results are incorporated into the simulation discussed below, assuming that the scale volume has a linear function of cumulative production.

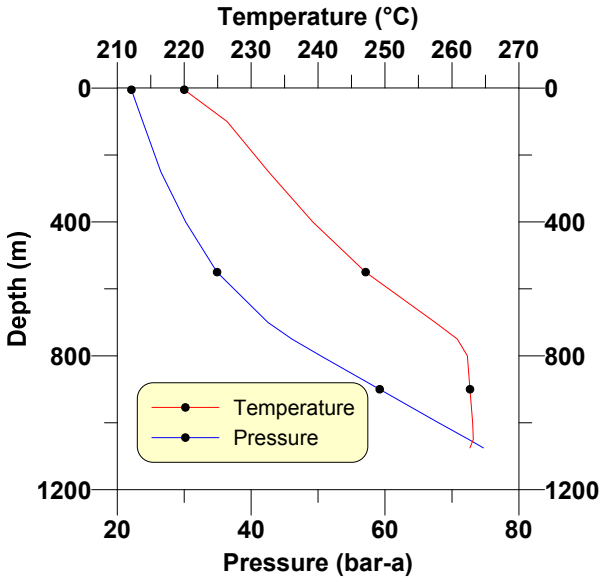

FIGURE 8: Well A-3 dynamic profiles at 42.5 kg/s (02/12/1987)

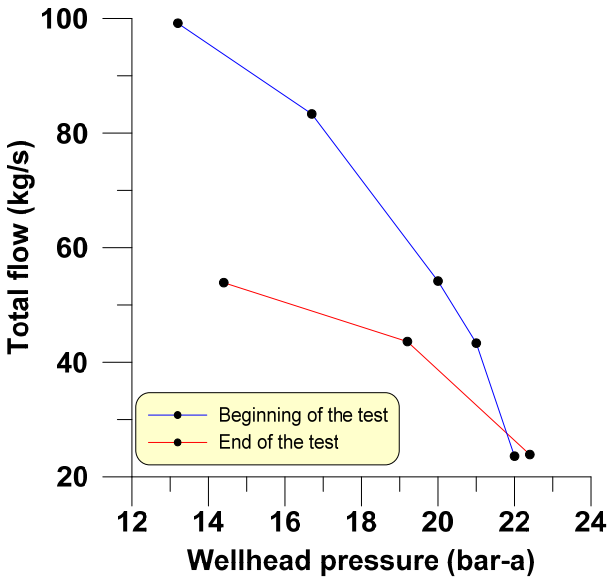

FIGURE 9: Wellhead output curves of well A-3 (Aquater, 1988)

Considering the results of the caliper log run at the end of the production period, a scale rate of about 1.0×10^{-8} $m^3/kg/s$ was determined. The internal diameter at a given time was then calculated according to the cumulative production at that time, considering constant scale thickness from the surface down to 870 m (Battistelli et al., 1991).

3.5 Wellhead output curves with time

Wellhead output tests were performed at the beginning of well A-3 testing and near the end of the long term of production. Comparison of the two wellhead curves reveals that a sizeable negative change in well output occurred during that period (Figure 9).

There was a decline in the well output during the long-term production test and the Caliper log. (Figure 10) and it appears that scale build-up is to blame for the decline over about a 3 month period. For a given wellhead pressure (WHP), the corresponding observed total mass flow rate decreases drastically for the lower WHP.

3.6 Reservoir pressure drawdown

Pressure recovery tests were carried out early and later in the 3.5 month long production test. They show a fast recovery at the beginning of the

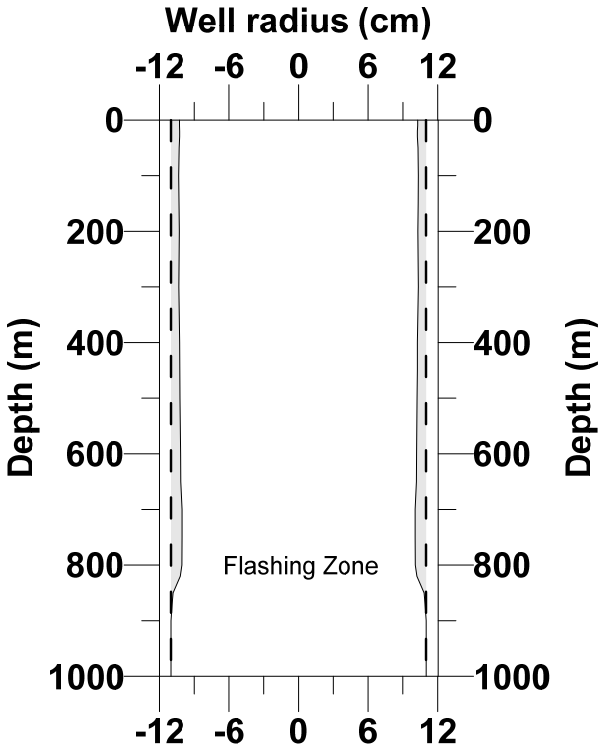

FIGURE 10: Caliper logs of well A-3

production test but slow at the end (Figure 11). This implies that a local, permanent reservoir drawdown of about 10 bars occurred between the two dates.

The reservoir pressure drawdown seen between September and December 1987 might be due to long term precipitation of salt water minerals, like anhydrite, making the reservoir's outer boundaries very tight with minimal natural recharge to the hot and permeable inner reservoir. Thus, it is likely that the Asal Rift reservoir pressure will decline rapidly at the beginning of production and only stabilise at high drawdown. Similar behaviour is seen in the Reykjanes field in Iceland (Sigurdsson, 2010). The Reykjanes behaviour, coupled with the observed reservoir pressure drawdown in well A-3, therefore suggests reinjection as a long term reservoir management strategy.

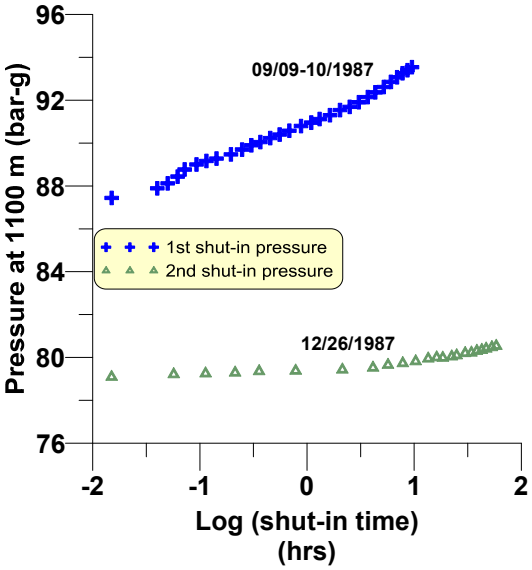

FIGURE 11: Pressure recovery curves at beginning (blue) and end (green) of 1988 flow tests (Aquater, 1988)

4. GEOCHEMISTRY AND SCALE DEPOSITION

The highly mineralised geothermal fluids encountered in a saline system like that in Asal, are subject to supersaturation. Successful operation of wells tapping such fluids is, therefore, strongly dependent on properly designing and implementing the right management strategy. One of the possibilities used for dealing with scales is to vary the depth of the flashing zone by adjusting the wellhead pressure to reduce the frequency of the mechanical scale removal of a well, and to insure that deposition is not occurring down in the open hole. Once it becomes known at what wellhead pressure the formation of scales is minimized, future wells should be developed with a perspective on the mitigation of the wellbore scale rate by having a production casing big enough to maximize the output of the well. This question is discussed in the following. Field case histories are from the Asal Rift and Reykjanes.

4.1 Generalities of silica deposition in geothermal fields

In hydrothermal areas silica deposition occurs at different depths in various forms. These include quartz, chalcedony, cristobalite, and amorphous silica. Quartz is the most stable form of silica, and has the lowest values of solubility. Deep geothermal water is usually in equilibrium with quartz at the prevailing reservoir temperature (Tassew, 2001). Deposition of quartz in wellbore and surface equipment is not a common problem, due to the slow rate of formation. Amorphous silica is, however, associated with changes in temperature of the geothermal water. This is when steam flashes out of the rising well and fluid cooling takes place. Deposition of amorphous silica from supersaturated water is, thus, an annoying scale when precipitated in surface equipment such as pipelines, separators, turbine nozzles, heat exchangers and re-injection wells. This is more troublesome in high-enthalpy geothermal fields as steam separation is taking place there and because of higher initial silica concentrations. In most fields, the steam separator is operated below the amorphous silica saturation line so as to avoid silica scaling in the pipelines and separator. Operation above the amorphous silica line will cause scaling but at very different rates, depending on the water composition, retention time and other factors (Tassew, 2001).

In high-enthalpy systems where scaling cannot be avoided, direct removal of solid deposits by reaming with a drilling rig from the zone of deposition is found effective if the deposition has not plugged the aquifers or the slotted liner portion of the well. Tests and experience also show that chemical inhibitors combined with pressure management methods can be applied to prevent the development of Galena (PbS) scales on wellbores in Asal (Virkir-Orkint, 1990).

4.2 Geochemistry of Asal wells

According to geochemical studies undertaken in the Asal Area (Correia et al., 1983), several groups of thermal springs have been identified: Manda Inakir and Korili springs, located in the eastern part of Asal; WadiKalou springs, located in the southern part of the Lake Asal; and Alifita and Eadkorar springs on the northern side of Asal.

Chemical analysis of the springs showed a relationship with sea water influx except for one, located in the southern part of Asal, in KalouWaddi. Other springs from the southern part and the northern part of the Lake showed mixing of the sea water and the lake water. The degree of mixing is more or less intense for each group of springs, according to the advancement of the reaction or to the interaction of varying proportions between water that has reacted intensely and sea water that has reacted poorly with basalt. It has been shown that the hyper-saline water of Lake Asal also contributes to the geothermal reservoir (Jalludin, 2011).

Table 2 shows the chemistry of several water samples collected from shallow aquifers in wells A-3 and A-6, and from Lake Asal. Mineralogical and isotopic studies in well A-2 have identified substantial water-rock interaction. Several estimations of the water/rock ratio have shown that zones of intense circulation exist. The upper part of the borehole is poorly altered in comparison to a rhyolite layer (at a depth interval of 300-600 m) and the lower parts of the borehole are indicative of substantial fluid circulation. Quartz, adularia, albite and epidote appear successively as a function of depth (Fouillac et al., 1989).

TABLE 2: Water composition in wells A-3 and A-6

Components	A3	A4	A5	A6	Lake Asal
pH	4,9	4,8	5,0	5,0	7,1
Na	37452	39839	13000	42000	101200
K	7273	6250	500	6000	5161
Ca	23928	20630	400	8532	2677
Mg	37	34	1500	700	12500
Cl	106000	103000	20000	52000	199155
SO4	32	12	2500	447	4320
SiO2	520	550	900		
HCO3	66	76	102	38	184
Li	31	17	33		6
F	7	4			
NH3	9,1	9,3			
Zn	3,1	5,6			
Pb	3,4	5,2			
Fe	6,7	4,4			

From the study (Virkir-Orkint, 1990) performed for comparison on collected samples from shallow aquifers in wells A-3 and A-6 and from Lake Asal, it appears that all aquifers encountered are mainly recharged by sea water.

4.3 Downhole scaling in well A-3

The production test performed on the productive wells A-3 and A-6 showed a high scale build up rate, both at the surface facilities as well as inside the wellbore, as shown by the caliper log (). The scale found in those wells mainly consisted of sulphides and silica. Sulphides start precipitating at temperatures close to those encountered at the downhole flashing zone, between 250 and 260°C, while silicas are present at a lower temperature of about 220°C. Decrease in well productivity with production

time was observed in well A-3. From the in-depth studies carried out, it was found that production decline was mainly due to frictional pressure losses within the wellbore caused by high relative roughness of a scale deposit (Aquater, 1988).

Conclusions from the drilling report on scaling problems encountered during the well test production performed in well A-3 and summarized in the final drilling report (Aquater, 1988) are:

- Calculated pH from the deep fluids indicates a rather acid condition, although compatible with the high content of Na and K.
- The measured amount of Fe was exceeded 4 to 6 times, for wells A-6 and A-3, respectively; the concentration was compatible with the equilibrium between the calculated H_2S and pyrite. This value is due to the aggressive action of brine which causes corrosion effects on the casing during its ascent.
- It was observed that, depending on the temperature at which sea water interacts with the surrounding rocks, as well as on the water-rock contact period, there is a difference in the ionic content of the fluids when compared with sea water.
- The water in Lake Asal is composed of very concentrated sea water, due to evaporation, and its $CaSO_4$ content is modified owing mainly to precipitation. Deep water seems to have no contact with Lake Asal waters and the Ca/Mg ratio is extremely different.
- Downhole fluids collected in well A-5 showed that the water at the centre of the rift has a much higher salinity than that on the borders.

Another study on scaling and corrosion in well A-3 was made by Virkir-Orkint (Virkir-Orkint, 1990) for the Djiboutian Electricity Company. The object of the study was the assessment of the scaling effect and corrosion on the wellbore and the determination of the optimum level of production for the well.

Table 3 shows the scale composition at the surface facilities of well A-3. A manifold was used for collecting samples at similar points of the facilities. A comparison of the analyses pointed out that the scale deposits were formed basically by the same elements. The only difference was the concentration of these elements due to the different Pb content. Laboratory chemical samples, taken at different points in the well, show a great difference between the scale compositions in the well.

TABLE 3: Chemical composition of scales from well Asal-3 (Ármannsson and Hardardóttir, 2010)

Constituent %	WH	OR	TP	SP	BP	SS	WB
P_0 bar	20	17.7	17.7	17.7	17.7	0	0
SiO2	19.6	0	6.7	40.7	30.5	56.4	72.9
Al2O3	3.7	0	1.0	4.3	3.4	8.6	2.7
Fe2O3	22.5	0	6.7	31.8	25.8	14.8	2.7
MnO	2.3	0	0.9	5.8	3.7	0.7	0.2
MgO	1.6	0	0.1	0.7	1.1	0.2	0.2
CaO	0.6	0	0.6	1.6	1.4	8.4	12.8
Na2O	4.4	0	0.3	1.4	1.7	8.1	0.8
K2O	0.1	0	0	0.7	0.4	1.9	2.9
S	13.7	14.9	18.3	4.0	8.0	0.2	0.4
Cu	0.4	0	0	0.1	0	0.1	0.1
Pb	22.3	85.1	65.4	7.2	23.3	0.2	0.4
Zn	8.8	0	0	1.7	1.0	0.4	0.1

WH: Wellhead; OR: Separator line orifice pressure (90 mm); TP: Two phase pipe separator line; SP: Separator; BP: Brine pipe; SS: Single-drum silencer; WB: Weir box.

A special chemical and corrosion facility was used to determine the scaling rates with variable wellhead pressure. Results are shown in Figure 12. At lower flowing wellhead pressure (<17 bars) the scale rate is 9.2cm/year with a predominant component of iron silicates ($FeSiO_3$). At wellhead pressures above 18

bars, the scaling rate dropped 6-fold and the predominant precipitate component was that of Galena (Virkir-Orkint, 1990).

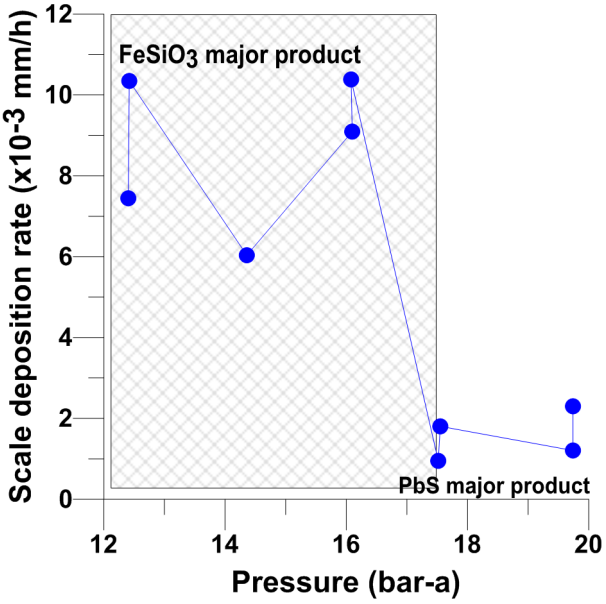

FIGURE 12: Scale deposition rates in well A-3 at different wellhead pressures (Virkir-Orkint, 1990)

During the scales studies (Virkir-Orkint, 1990) in well A-3, two types of inhibitors developed by Nadar Chemical Company, based in Italy, were tested for sulphide inhibition, i.e. a sequestration agent for heavy metals (type Nadar 4093) and a sequestration and dispersing agent used against magnesium salts and silica (type Nadar 1008). Both inhibited metal sulphide formation. The former caused iron silicate formation and was deemed unsuitable; but the latter caused the formation of calcium chloride, which could be avoided by acidification, but corrosion problems still have to be resolved. Sodium formates have been used as reducing agents (Gallup, 1993) to control ferric silicate deposition, and it was found that the formate also mitigates against acid corrosion. As has been observed, the extent of iron silicate scaling in well A-3 is small above 16-18 bar-a; the recommendation is to keep the wellhead pressure above this value during discharge at flowing pressures (Ármannsson and Hardardóttir, 2010).

4.4 Comparison between scaling rates in Reykjanes and Asal

The Icelandic geothermal field of Reykjanes is known to have similar behaviour as in Asal in terms of host rock and fluid. In order to better understand the scaling problems in Asal, comparison on scaling rates was made between these two fields. The scale deposit rates in the two fields were compared for wells RN-9, RN-10 and RN-11 in Reykjanes, and well A-3 in Djibouti.

Figure 13 shows the scaling rate in wells RN-9, RN-10 and RN-11 in Reykjanes. The scale deposit rate has increased as a function of decreasing sample pressure. However, although the scaling thickness measurements were not very accurate due to the rustiness of the iron coupons used for the collection of the scaling component, they will be used as a first approach in order to compare the scaling rates to what were obtained in Asal wells. From the Reykjanes wells, it can be said that at higher pressures the scale rate is around 5 mm/year, and at pressure below 15 bars, the scale rate is more or less double (Hardardóttir et al., 2005).

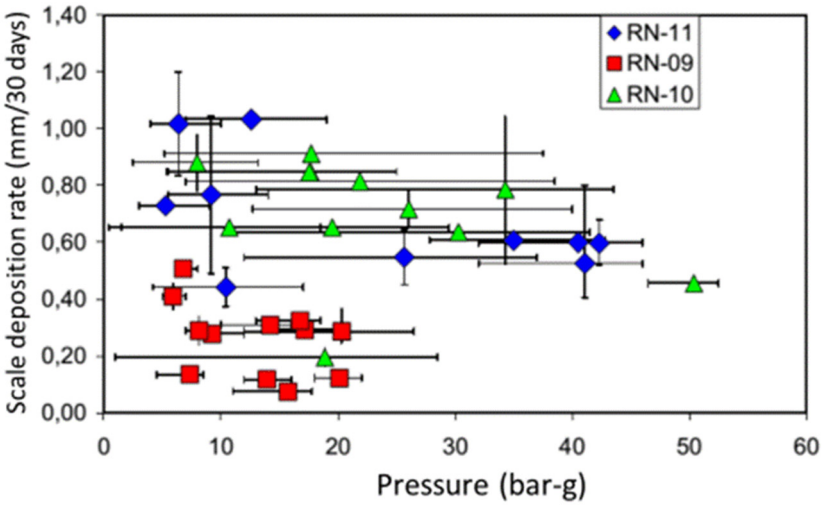

FIGURE 13: Rate of scaling in experiments in wells RN-9, RN-10, RN-11 (Hardardóttir et al., 2005)

Figure 14 summarizes the comparison on scale deposition rate between Asal and Reykjanes fields. It can be seen that for higher wellhead pressures the scale rate is at its minimum for both fields.

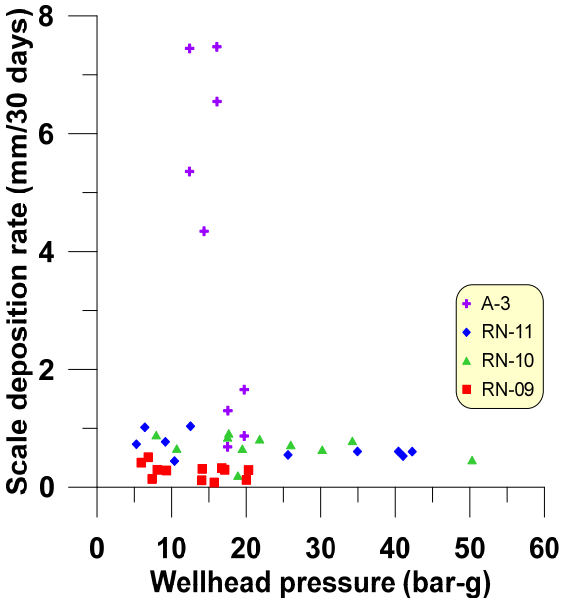

FIGURE 14: Comparison of thickness scale rate in Reykjanes wells and in Asal well A-3

5. NUMERICAL WELLBORE MODELLING

The discussion above shows that the salty reservoir fluid encountered in the Asal Rift and elsewhere is far from easy to manage. Negative impact on the wellbore diameter and total flow can be particularly severe if care is not taken in operating these wells at the right wellhead pressure. The central part of the work done here is, therefore, to use the available downhole data on well A-3 to calibrate a well-reservoir model for a typical well in the Asal Rift. With such a model at hand, its three most sensitive parameters, i.e. wellbore diameter, feedzone pressure and feedzone enthalpy, can be studied for likely wellhead output curves. The goal is to identify which parameters can best help in ensuring future wellhead operating pressure being comfortable above the 18 bars threshold shown in Figure 12. Also, the study will look at the impact of having the slow but continuous ~3 cm/year cumulative scaling rate in new wells at a wellhead pressure above 18 bars and how that behaviour may impact well diameter design strategy and drilling targets. For clarity, the analysis is split into two sections. First, 18 scenarios of well output for new and scaling free wells is studied, while the latter section looks at the time impact of cumulative downhole scaling build-up, which unfortunately negatively impacts the total steam and brine coming from a well over time.

5.1 The wellbore simulator Hola

The wellbore simulator Hola is used for generating output curves for well A-3 in the following steps. HOLA reproduces the measured pressure and temperature profiles in a flowing well and determines the thermodynamic properties of the water, and the relative flow rates at each feedzone for a given discharge condition at the wellhead (Björnsson and Bödvarsson, 1987). It has two approaches, summarized in Option 1 and Option 2 of the wellbore flow simulation. Option 1 needs known discharge conditions at the wellhead (pressure, flow and enthalpy), in addition to flow rates and enthalpies of all but the deepest feedzone. The simulator proceeds from wellhead to bottomhole to calculate the flowing temperature and pressure profile along the well. In Option 2, the user specifies the required flowing wellhead pressure and bottomhole pressure and for each feedzone, the productivity indices and properties of the reservoir fluid pressure and enthalpy. The simulator then proceeds from bottomhole to wellhead to calculate the expected wellhead output (wellhead enthalpy, flowrate, temperature, and phase composition) for the required wellhead pressure.

The flow of fluid in a geothermal well can be represented mathematically by two sets of equations. Between the feedzones, the flow is represented by: one-dimensional steady-state momentum, energy and mass flux balances, which are:

- Mass balance:

$$\frac{d\dot{m}}{dz} = 0 \qquad (1)$$

- Momentum balance: The total pressure gradient is the sum of the friction gradient, acceleration gradient and fluid elevation potential.

$$\frac{dp}{dz} - \left[\left(\frac{dp}{dz}\right)_{fri} + \left(\frac{dp}{dz}\right)_{acc} + \left(\frac{dp}{dz}\right)_{pot}\right] = 0 \quad (2)$$

- Energy balance:

$$\frac{dE_t}{dz} \pm Q = 0 \quad (3)$$

where $\dot{m}$ is the total mass flow, P is pressure, E_t is the total energy flux in the well and z is the vertical depth coordinate. Q denotes the ambient heat loss over a unit distance. The plus and minus signs indicate downflow and upflow, respectively.

Between the well and the reservoir, the governing equation is:

$$\dot{m}_{feed} = PI\left[\frac{K_{rl}\rho_l}{\mu_l} + \frac{K_{rg}\rho_g}{\mu_g}\right](P_r - P_w) \quad (4)$$

where $\dot{m}_{feed}$ is the feedzone flowrate, PI is the productivity index of the feedzone, k_r is the relative permeability of the phases (subscripts l for liquid and g for steam), μ is the dynamic viscosity, ρ is density, P_r is the reservoir pressure and P_w is the pressure in the well.

The relative permeabilities are here calculated by linear relationships ($K_{rg} = S$ and $K_{rl} = 1 - S$, where S is the volumetric steam saturation of the reservoir) (Björnsson et al., 1993).

6. CALIBRATING A NUMERICAL WELLBORE MODEL FOR WELL A-3

6.1 Wellbore geometry

The present work uses flowing downhole data in well A-3 as a basis for a general complete reservoir-well model. The well was drilled in 1987 at the southwest border of the Asal Rift to1316 m depth (Figure 3FIGURE 3). The casing design of well A-3 consists of a 20" diameter surface casing to a depth of 192 m, 13⅜" diameter for the anchor casing between 192-397 m, 9⅝" diameter for the production casing from 1016 m up to the surface, and an open hole below that down to 1316 m (Figure 15). The well intersects its main feed zone at 1075 m depth, characterized by a temperature and pressure of around 258°C and 80 bars, respectively.

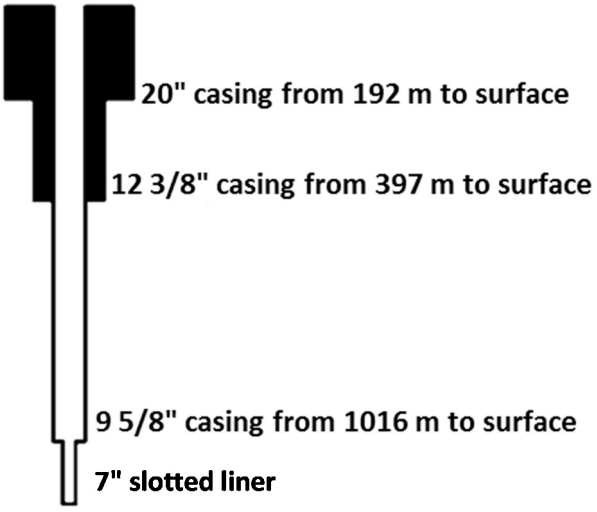

FIGURE 15: Casing design of well A-3

At the wellhead, the fluid has a high scaling nature with a weir box salinity of 180 g/l of NaCl and low gas content. The reservoir fluid is a single-phase liquid with high salinity content (115 g/l of NaCl) and a temperature range between 259 and 265°C (Aquater, 1988).

Analysis of pressure and flow variations, which occurred during the long term production test, indicate that the observed production decline is mostly due to the high rate of scaling in wellbore. The following

chapters of this report will focus on analysing the scaling in the wellbore, using the wellbore simulator "Hola", calibrated against existing field data for well A-3.

6.2 Estimating the well productivity index

The second mode of Hola is used to calibrate a numerical model for well A-3, in particular the productivity index (PI) described above. The default productivity index proposed by the software is first used as an initial guess for the reservoir and adjusted after iteration in order to fit the simulated output flow with the observed one. This was done for all the downhole data shown in Figures 6-8. This is summarized in Table 4TABLE.

TABLE 4: Estimated productivity indices for well A-3

Day	Date	Productivity index (m^3)	Flow (kg/s	Wellhead pressure (bar-a)
1	09/04/1987	1.155×10^{-11}	26.3	21.5
2	10/14/1987	0.750×10^{-11}	49	20
3	12/02/1987	0.810×10^{-11}	42.5	19.4

The numerical models are calibrated against field data collected on three different dates (see Table 4). The first output date from Day 1 corresponds to the beginning of the production test, while Day 3 corresponds to the end.

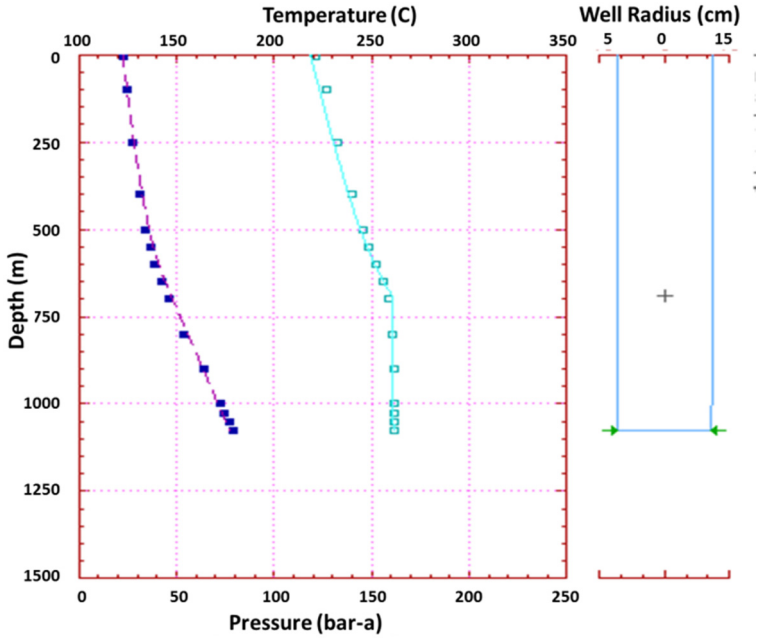

FIGURE 16: Model calibration from Day 1

Figures 16 and 17 show the match between the simulated temperature and pressure profiles from Hola wellbore simulator, with the measured ones recorded on the left based on output from the first day (Day 1) and the right side near the last day (Day 3) of the production test period. Field data from Day 1 demonstrate good matches for both the pressure and temperature profiles. These data have been used for estimating the productivity index (Table 4) which is the only model parameter required by the numerical modelling for the next steps of our studies. Measured data from Day 1 were 78.1 bars and 261.2°C for the pressure and temperature at 1075 m depth, respectively. The match was obtained by using a default steel pipe roughness value of 5×10^{-4} m from the surface down to the bottom of the well. From Day 3, the observed bottomhole pressure and temperature used for the calibration were 78.1 bars and 261.2°C. The match was obtained by using a roughness value of 5×10^{-4} m from the surface down to the bottom.

The pressure and temperature profile matches were obtained for a reservoir productivity index of 1.55×10^{-11} m^3 and 8.1×10^{-12} m^3 for Day 1 and Day 3, respectively. The modelled productivity index of the reservoir decreased (Table 4) in the 3.5 month period between these two dates. The productivity index of the reservoir is, however, constant with the flow rate in most of the wells in the liquid phase.

The calibrated data from Day 1 to 3, as well as all the collected dynamic field data for well A-3, show a drop in pressure at the wellhead and at the feedzone of around 5 bars.

Figure 18 shows the calculated wellhead output curves of the well on the three dates. As stated in the previous section, the well has to be maintained at a high wellhead pressure of above 20 bar-a in order to minimize scaling inside the wellbore. The grey hashed part of Figure 18 is not considered for well A-3 because of the high scaling corresponding to the wellhead pressure values.

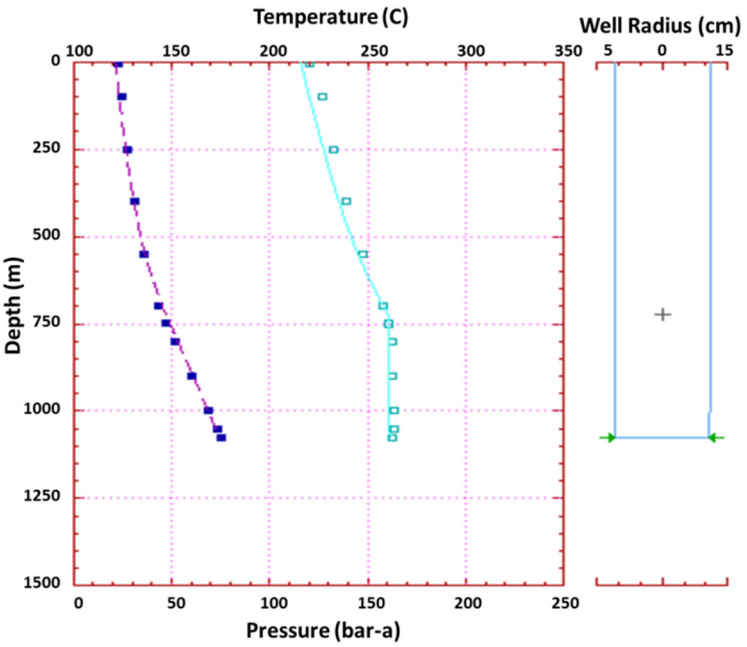

FIGURE 17: Model calibration from Day 3

For a reference constant WHP of 20 bar-a, a decrease in the mass flow of 17 kg/s was observed from Figure 18 between the beginning and the end of the 3.5 month production test. The decrease can probably be interpreted as an indication of reduction in well diameter which occurred during that period due to scale deposition. Diameter reduction from the flashing point to the top of the well shown by the caliper log (Figure 9) could explain the decline in well output due to a reduction in well radius due to scale deposition.

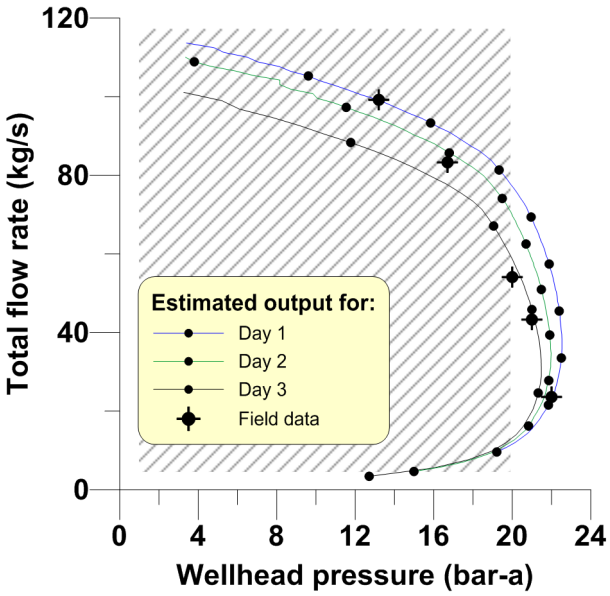

FIGURE 18: Predicted clean well output curves and measured output data for well A-3

7. PREDICTING CLEAN WELL OUTPUT CURVES

The use of wellbore simulator HOLA to assess the possible benefits of drilling larger, hotter and for higher pressure is discussed below. Well A-3 is already drilled with a 9⅝" production casing and 7 " liner. The proposed large well design involves a 13⅜" production casing and a 9⅝"for the liner. The proposed study aims to characterize the effects of pressure and enthalpy variation in wellbore on the output curves of the well. Output prediction and analysis are performed with the simulator for two different production casings: a standard casing of 9⅝" and a large production casing of 13⅜".

The study simulated a range of typical feed responses, summarized by Table 5, for both the standard well and the proposed new larger well design, in order to predict and compare the relative production that might occur in the wells in the future. The standard and large well designs have both been modelled as having a production casing shoe at 1075 m.

TABLE 5: Scenarios used for predicting well output

	Pressure (bar-a)	Temperature (°C)	Enthalpy (kJ/kg)	Casing 1	Casing 2
				9 ⅝"	13⅜"
				Scenario	
Pressure 1	80.3	260	1126	A1	A2
		280	1227.4	A3	A4
		300	1335	A5	A6
Pressure 2	70.3	260	1126	B1	B2
		280	1227.4	B3	B4
		300	1335	B5	B6
Pressure 3	60.3	260	1126	C1	C2
		280	1227.4	C3	C4
		300	1335	C5	C6

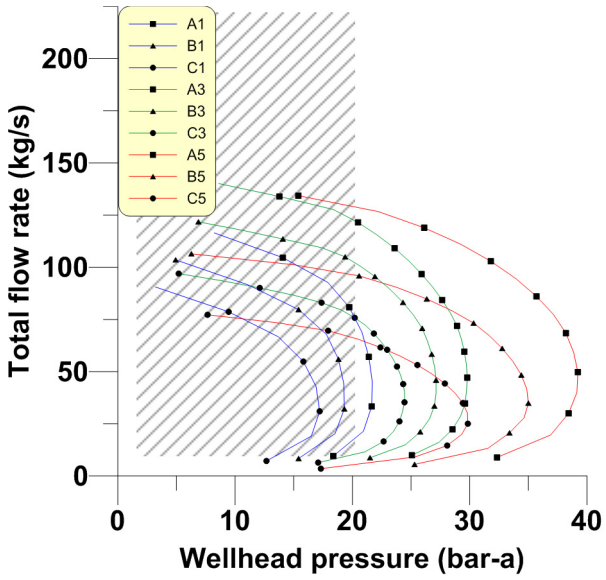

FIGURE 19: Clean well output curves for standard casing design

For each value of the feedzone pressure, three scenarios of enthalpy were simulated for the two casings which describe a combined effect on reservoir characteristics (fall in reservoir pressure and enthalpy variation in the reservoir).

Figure 19 shows the results of the standard casing to the simulation. The numerical model of the standard well was calibrated under a typical feed enthalpy of 1126 kJ/kg (260°C) for a measured reservoir pressure of 80.3 bar-a, which corresponds to scenario A1 in Table 5. Predicted output curves in the required range of wellhead pressure (20 bar-a, or above) from the simulator indicates that a maximum flowrate of around 110 kg/s can be obtained according to those characteristics. The maximum output for this normal casing, assuming a required wellhead pressure of 20 bar-a, is obtained for a total flow rate of about 135 kg/s for a feedzone temperature at 300°C.

Figure 20 shows the results of the large well to the simulation. A representative large design well was modelled with the actual characteristics of the well, assuming a typical feedzone enthalpy of 1126 kJ/kg and a reservoir pressure of 80.3 bar-a, corresponding to scenario A2. Predicted output curves in the required range of wellhead pressure (20 bar-a, or above) from the simulator indicate that a maximum flowrate of around 220 kg/s can be obtained according to those characteristics. The maximum output scenarios for this casing, assuming a required wellhead pressure of 20 bar-a, is obtained in scenario A6.

Comparison made on well output between the standard and large casings is plotted in Figure 21. The results demonstrate a real increase in well output in the range of aimed wellhead pressure if the large diameter well is selected. At a particular given wellhead pressure, the results from the simulation infer that the well outputs are doubled by the large diameter well. The results also show the effect of the casing on the wellhead pressure, allowing a discharge at very high wellhead pressures, up to 39 bar-a. This indicates that using a 13⅜" production casing will considerably improve the production of the well.

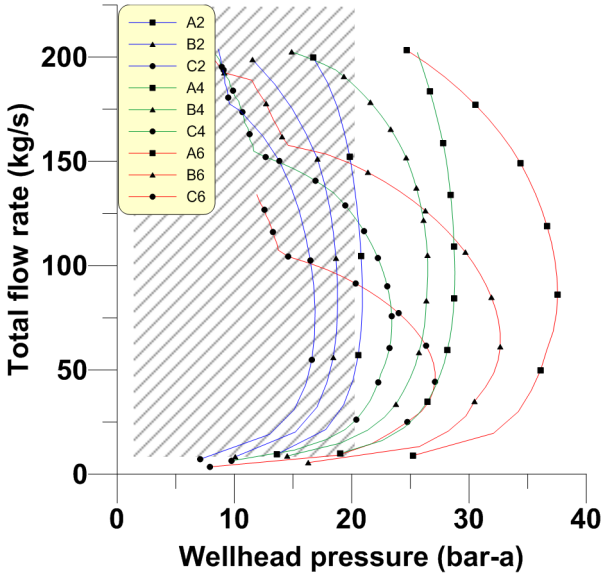

FIGURE 20: Clean well output curves for large casing design

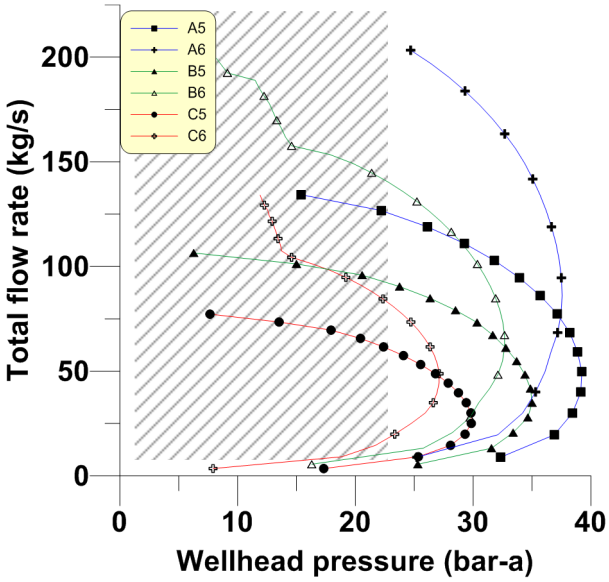

FIGURE 21: Comparison of wellhead output curves

8. MITIGATING IMPACTS OF LONG-TERM SCALING DEPOSITION

It is of interest to couple the gradual scale build-up in Asal wells at wellhead pressure above 20 bars to computed output curves. Table 6 shows how standard well diameter may change with time. Figure 22 shows and then describes computed wellhead output curves of the standard casing of well A-3. An observed reduction in wellbore diameter from 870 m up to the surface of the well of 3 cm/year (Aquater, 1988) is assumed. All the other characteristics of the well are considered as constant in order to emphasize the induced effect of scaling deposition on well output. Table 6 shows calculated well diameter, assuming the effect of scaling deposition on the wellbore for the actual casing of the proposed well.

TABLE 6: Wellbore diameter reduction due to scaling in the standard well

Time (year)	Casing 9⅝"	
	Scale diam. (m)	Well diam. (m)
0	0	0.22
1	0.0325	0.1875
	0.0650	0.155
3	0.0975	0.1225
4	0.130	0.09
5	0.163	0.057

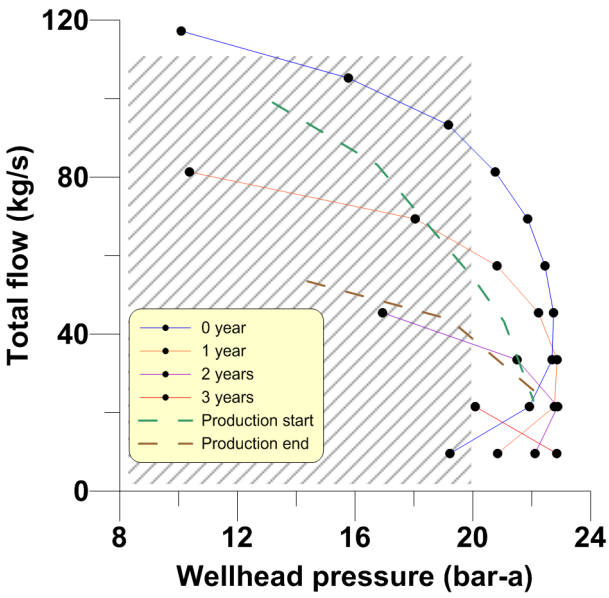

FIGURE 22: Measured and predicted output curves for standard casing in well A-3 and a 260°C feedzone

As previously stated, the scale deposition in the wellbore is pressure dependent. One way to deal with the scaling in the wellbore is to keep the well at a wellhead pressure above 20 bars. In the following studies, only the portion of the wellhead output curves above 20 bars is considered. Well output curves at high wellhead pressure for the standard casing (Figure 22) show that the well

output seems to be strongly impacted by scaling deposition in the wellbore. The plotted field data (red and green dashed lines in Figure 22), along with the simulated data, show that the well which has flowed before the production test seemed to have a scale deposit in the wellbore even before the production test.

Assuming a scale deposition in the wellbore, the well output curves of the new large diameter casing designed for well A-3 are described in Figure 23. An observed reduction on wellbore diameter from 870 m up to the surface, equivalent to 3 cm/year (Aquater, 1988), is assumed. All the other characteristics of the well are assumed constant in order to emphasize the induced effect of scaling deposition on well output. Table 7 shows estimated well diameter while assuming the effect of scaling deposition in the wellbore for the proposed well.

TABLE 7: Wellbore diameter reduction due to scaling in the large well

Time (year)	Casing 13⅜"	
	Scale diam. (m)	Well diam. (m)
0	0	0.32
1	0.0325	0.2875
2	0.0650	0.255
3	0.0975	0.2225
4	0.130	0.190
5	0.163	0.157

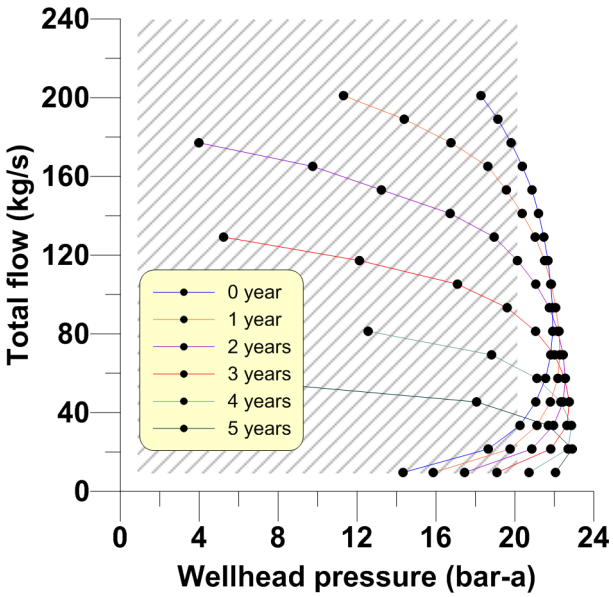

FIGURE 23: Scaling impact on a large casing well over time

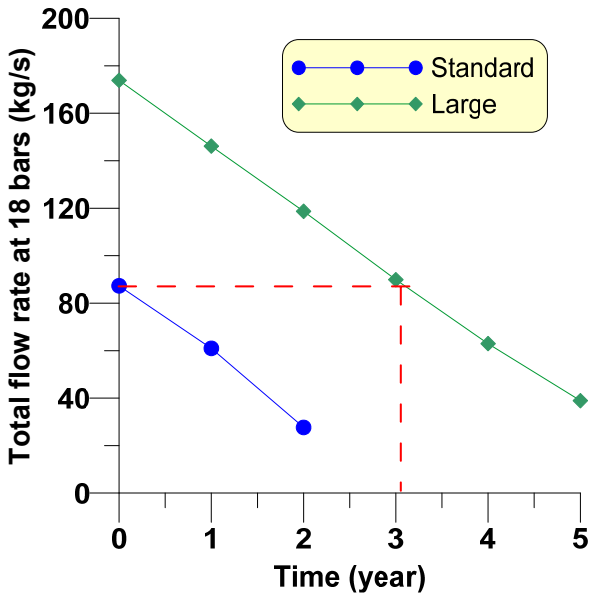

FIGURE 24: Effect of scale deposition with time on wellhead pressure at 18 bar-a

Figure 24 shows wellhead output curves at high wellhead pressure for the two casing designs. The figure shows that the well output is strongly impacted by scaling deposition in the wellbore. The plot of the well's output curves shows that the initial output flow predicted for the standard casing corresponds to the predicted output flow of the large casing well after 3 years of discharging at 18 bar-a. The initial output flow of the wells at high pressure (18 bars) is doubled by using a large casing (from 82 kg/s to 175 kg/s). One of the major benefits that can be obtained from a large design well, and emphasised clearly in Figure 24, is that after 3 years of 3 cm/year cumulative scaling, a standard well is nearly clogged while a large well is still flowing like a clean standard well. Despite the fact that the scaling cannot be completely eradicated from the well, an alternative management point of view could be developed from this casing; the frequency of mechanical cleaning operations or inhibitor operations might be reduced.

9. NEW WELL LOCATION AND DISCUSSION

The predicted wellhead output curves in Figures 19 and 20 show a very positive impact of raising the reservoir temperature being tapped by both well designs. It is, therefore, of interest to see if the existing temperature data collected in wells A-1 to A-6 can be used to propose an alternative new well location in the Asal Rift.

A proposed new large diameter well should be located between existing wells A-3 and A-4 (Figure 25). The new well will be drilled down to 2000 m via directional drilling in order to intersect both of the higher temperature areas next to well A-4 while also having the option of tapping the productive reservoir of well A-3. Such a decision is, however, a multidisciplinary operation and a sizeable pool of expertise is needed for a proper decision on the final well design and azimuth.

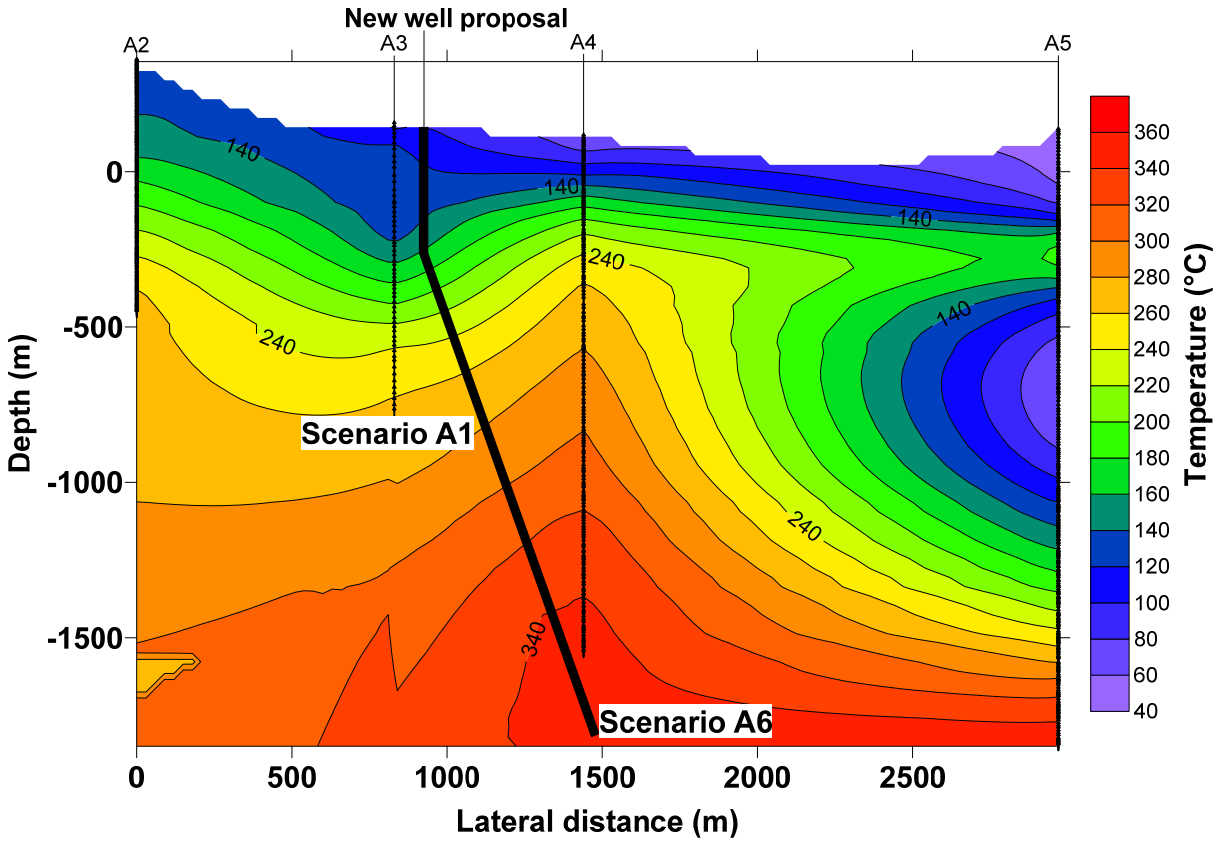

FIGURE 25: Temperature cross-section of Asal and proposed new well location

A nominal design of the new well might be:

- Total depth: 2000 m;
- Surface casing: 24";
- Anchor: 18⅝";
- Production casing: 13⅜";
- Slotted liner: 9⅝".

10. CONCLUSIONS AND RECOMMENDATIONS

A long term production test conducted during the first and second Djibouti drilling campaigns in 1975 and 1987 constitute the background of this study. Numerical modelling and analysis of predicted output curves for Asal wells is based on a large quantity of available field data collected during that period.

Tests made on well A-3 show a pressure dependent scaling build-up of iron silicates ($FeSiO_3$), and galena (PbS) at lower and higher wellhead pressure, respectively. The results indicate a high scaling rate of 9.2 cm/year at the lower pressure which drops 6-fold at higher wellhead pressure (Virkir-Orkint, 1990). Reservoir pressure drawdown was observed from the collected data, probably due to salt precipitation, suggesting the need for reinjection.

Mode one and two of Hola Wellbore Simulator, calibrated with existing field data, was used for output predictions and show a good match for both temperature and pressure. A high productivity index, modelled for the reservoir, indicates the presence of a highly permeable feedzone in the vicinity of well Asal 3 at about 1075 m depth.

A new well was modelled to assess the possible benefits of drilling for a large diameter casing and liner, by using the simulator Hola, and then studied under 18 scenarios of various pressure and enthalpy for both standard and large casings. The study showed a reservoir dominated flow for well A-3 limited by wellbore diameter which indicates that using a large production casing in Asal would considerably improve the output at high wellhead pressure.

Modelled output flow of an Asal well at high wellhead pressure was doubled by using a large casing. After 3 years of 3 cm/year of cumulative scaling, the standard well was nearly clogged while the large well was still flowing like a new and clean standard well.

Directional drilling is proposed for a new well in Asal and it might be drilled between wells A-3 and A-4 down to 2000 m in order to intersect better enthalpy.

ACKNOWLEDGMENTS

The preparation and writing of this report faced many challenges. In particular, understanding in a short time what was done in 40 years of geothermal exploration in our main geothermal field in Djibouti. It has been possible with the unqualified help of my supervisor, Mr. Grímur Björnsson. I owe him my first and sincere appreciation for his helpful guidance and excellent advice during the preparation of this report.

I would like to address my thanks to Mr. Lúdvík S. Georgsson, the Director of the United Nation University, and to Dr. Ingvar Birgir Fridleifsson, the former Director as well as to our Director Managers, Mr. Abdourahman Haga, Mr. Bouh Moussa and Mr. Abdou Mohamed, for allowing me this opportunity to study here in Iceland and for their full support in my work.

I am very grateful to all the UNU staff, Mr. Ingimar G. Haraldsson, Ms. Thórhildur Iceberg, Ms. Frída Ómarsdóttir, Ms. María S. Gudjónsdóttir, and Mr. Markús A.G. Wilde, for providing all the necessary facilities which made my stay in Iceland comfortable and conducive to learning.

Special thanks go to Ms. Svanbjörg, Mr. Halldór Ármannsson and Ms. Vigdís Hardardóttir, who gave me important guidance through their research. Their ideas and concepts have had a remarkable influence on my work. Also, I want to thank all the ISOR staff for their assistance at all times.

Finally, I must express my gratitude to my colleagues, the UNU-GTP-2014 Fellows, for their amity. Special thanks and good luck to the reservoir engineers.

REFERENCES

Aquater, 1988: *Asal 3 final report.* Aquater, Djibouti, report (in French).

Ármannsson, H. and Hardardóttir, V., 2010: Geochemical patterns of scale deposition in saline high temperature geothermal systems. *Proceedings of the 13th International Symposium on Water-Rock Interaction, Guanajuato, Mexico. Taylor and Francis Group, London*, 133-136.

Árnason, K., and Flóvenz, Ó.G., 1995: Geothermal exploration by TEM-Soundings in the Central Asal Rift in Djibouti, East Africa. *Proceedings of the World Geothermal Congress 1995, Florence, Italy,* 933-938.

Battistelli, A., Rivera, J., and Ferragina, C., 1991: Reservoir engineering studies at the Asal field. Republic of Djibouti. *Geothermal Resources Council, Bulletin, Nov. 1991*, 280-289.

Björnsson, G., and Bödvarsson, G.S., 1987: A multi-feedzone wellbore simulator. *Geoth. Res. Council, Transactions, 11*, 503-507.

Björnsson, G., Arason, P., Bödvarsson, G.S., 1993: *The wellbore simulator HOLA. Version 3.1.* User's guide. Orkustofnun, Reykjavík, 36 pp.

BRGM, 1975: *French territory of Afars and Issas: Final report of survey.* BRGM, France, report (in French).

BRGM, 1980: *Testing of geothermal fluids. Lake Asal (Republic of Djibouti).* BRGM, France, report (in French).

Correia, H., Demange, J., Fabriol, R., Gérard, A., Varet, J., 1983: *The Asal geothermal field, summary of data available on January 1, 1983.* BRGM, France, report BRGM/83-SGN-022-GTH (in French), 71 pp.

D'Amore, F., Guisti, D., and Abdallah, A., 1997: Geochemistry of the high-salinity geothermal field of Asal, Republic of Djibouti. *Geothermics, 27,* 197-210.

Elmi, D., 2005: Analysis of geothermal well test data from the Asal Rift area in the Republic of Djibouti, Iceland. Report 6 in: *Geothermal training in Iceland 2005*. UNU-GTP, Iceland, 39-59.

Fouillac, A.M., Fouillac, C., Cesbron, F, Pillard, F., Legendre, O., 1989: Water-rock interaction between basalt and high salinity fluids in the Asal Rift. *Chemical Geology, 76*, 271-275.

Gallup, D.L., 1993: The use of reducing agents for control of ferric silicate scale deposition. *Geothermics, 22-1,* 39-48.

Haga, A.O., Youssouf, S.K. and Varet, J., 2012: The Manda-Inakir geothermal prospect area, Djibouti. P*roceedings of the ARGeo-C4 Conference, Nairobi*, 9 pp.

Hardardóttir, V., Ármannsson, H. and Thórhallsson, S., 2005: *Characterization of sulfide-rich scales in brine at Reykjanes. Proceedings of the World Geothermal Congress 2005, Antalya, Turkey*, 8 pp.

Hjartarson, G., Gísladóttir, V., Gíslason, G. and Ólafsson, K., 2010: Geothermal development in the Asal Area, Djibouti. *Proceedings of the World Geothermal Congress 2010, Bali, Indonesia,* 8 pp.

Jalludin, M., 2003: An overview of the geothermal prospections in the Republic of Djibouti. Results and perspectives. *Proceedings of the 2nd Kenya Electricity Generating Company Geothermal Conference 2003, Nairobi- Kenya.*

Jalludin, M., 2011: State of knowledge of geothermal provinces in Asal. *Presented at Short Course VI on Exploration for Geothermal Resources, organized by UNU-GTP, KenGen and GDC, Naivasha,* 17 pp.

Jónsson, Í., 1985: Republic of Djibouti - country report. In: *Geothermal exploration project.* Institute Superieur d'Etudes et des Recherches Scientifiques et Techniques, Djibouti, 175-178.

Marinelli, G., and Varet, J., 1973: *Structure and evolution of the Sud fo "Host Danakil".* French Territories of Afar, Issas and Ethiopi, report, 1119-1122.

MERN, 2004: *Project-pipeline proposal for implementation under ARGeo.* Djibouti, report.

Omenda, P.A., 2008: Geothermal activity of the East African Rift. *Presented at Short Course III on Exploration for Geothermal Resources, organized by UNU-GTP and KenGen, Naivasha,*12 pp.

Sigurdsson, Ó., 2010: The Reykjanes seawater geothermal system – its exploitation under regulatory constraints. *Proceedings of the World Geothermal Congress 2010, Bali, Indonesia,* 8 pp.

Smithonian Intsitution, 2013: Global Volcanism Program, website: *www.volcano.si.edu/gyp/*

Tapponier, P. and Varet, J., 1974: *The Mak'arrasou area in Afar: Equivalence to oceanic transform faults.* Academy of Science, Paris, report (in French).

Tassew, M., 2001: Effect of solid deposition on geothermal utilization and methods of control. Report 13 in: *Geothermal training in Iceland 2005*. UNU-GTP, Iceland, 291-310.

Virkir-Orkint 1990: *Djibouti. Geothermal scaling and corrosion study.* Virkir-Orkint, Reykjavík, report, 109 pp.